



Cite this: RSC Adv., 2016, 6, 101688

## Biocompatible titanate nanotubes with high loading capacity of genistein: cytotoxicity study and anti-migratory effect on U87-MG cancer cell lines

Tarek Baati,<sup>\*a</sup> Bochra Bejaoui Kefi,<sup>b</sup> Aicha Aouane,<sup>c</sup> Leila Njim,<sup>d</sup> Florence Chaspoul,<sup>e</sup> Vasile Heresanu,<sup>f</sup> Abdelhamid Kerkeni,<sup>g</sup> Fadoua Neffati<sup>h</sup> and Mohamed Hammami<sup>a</sup>

Titanate nanotubes (Ti-Nts) have proved to be a potential candidate for drug delivery due to their large surface change and higher cellular uptake as a direct consequence of their tubular shape. Ti-Nts were assessed for their safety, their kinetics of cellular uptake on U87-MG cell line and for genistein loading efficiency. No cytotoxic effect was observed under higher empty Ti-Nts concentrations up to 100 µg mL<sup>-1</sup>. The multiwalled tubular morphology was found to be an important parameter promoting high drug loading. The Ti-Nts could achieve higher genistein drug-loading content (25.2%) and entrapment efficiency (51.2%) leading to a controlled drug release as well as a higher cellular uptake of genistein-loaded-Ti-Nts which induces higher cytotoxicity and significant anti-migratory effect on U87-MG human glioblastoma astrocytoma, promising efficient antitumor activity.

Received 2nd October 2016  
Accepted 19th October 2016

DOI: 10.1039/c6ra24569b  
[www.rsc.org/advances](http://www.rsc.org/advances)

### Introduction

Glioblastoma is the most common primary malignant brain tumor, accounting for about 20% of all primary brain tumors in adults and it is also called grade IV astrocytoma.<sup>1</sup> Glioblastoma is aggressive and characterized by rapid cell growth and local spread. Despite the major progress in the development of chemotherapeutic drugs and improved techniques for surgery and radiotherapy, glioblastoma prognosis remains poor with a median survival of 15 months.<sup>2</sup> Genistein, (4',5,7-trihydroxyisoflavone), a small, biologically active flavonoid, is identified as the predominant isoflavone in soy products.<sup>3,4</sup> Epidemiological studies suggest that genistein helps to protect against cancer including glioblastoma.<sup>5-9</sup> Indeed genistein is potential therapeutic agent for induction of apoptosis in human glioblastoma cell lines T98G and U87MG through triggered oxidative damage.<sup>10</sup> Likewise genistein was observed to inhibit cancer spreading cells in two of the three glioblastoma cancer

cell lines including U87-MG glioblastoma in a dose-related manner.<sup>11,12</sup> The major limitations of chemotherapy for treatment of glioblastoma are the inability of many drugs to pass through the blood-brain barrier and their low efficacy for induction of apoptosis. Although genistein has been shown to cross the blood-brain barrier to a certain extent,<sup>13,14</sup> its clinical effectiveness in glioblastoma treatment has been limited by a very short half-life after systemic delivery due to the blood deaminases rapid metabolism which limits drug exposure to brain tumor cells. In the light of these limitations, high drug doses are needed to reach therapeutic drug concentrations within brain tumors after intravenous delivery, resulting in systematic side effects. Moreover the low aqueous solubility of genistein is presumably related to its low bioavailability. Hence, increase the passage of a drug through the blood-brain barrier without toxic effects is a challenge. The application of nanotechnology in medicine is becoming increasingly popular.<sup>15-19</sup> There is a substantial interest in developing therapeutic options for glioblastoma treatment based on the use of nanoparticles formulations. Interestingly this novel technology helps to overcome the lack in conventional chemotherapeutic drugs specificity, as well as, it enhance the early detection of precancerous and malignant lesions. Generally, a perfect drug nanocarrier system should have several characteristics including stable structure, high drug encapsulation efficiency, high cellular uptake, more desirable biodistribution and more reasonable pharmacokinetics as well as selectively accumulate at the tumor site through the enhanced permeability and retention (EPR) effect.<sup>20,21</sup> Recently

<sup>a</sup>Laboratoire des Substances Naturelles, Institut National de Recherche et d'Analyse Physico-Chimique (INRAP), technopole Sidi Thabet Ariana 2020, Tunisie. E-mail: tarek.baati@gmail.com; Tel: +216 71 537 666; +216 54 098 502

<sup>b</sup>Département de Chimie, Faculté des Sciences de Bizerte et INRAP, Tunisie

<sup>c</sup>Centre de Microscopie électronique, IBDM Campus de Luminy, Université Aix Marseille, France

<sup>d</sup>Service d'Anatomie Pathologique, CHU de Monastir, Tunisie

<sup>e</sup>CNRS, IRD, IMBE, Université Aix Marseille, Université Avignon, France

<sup>f</sup>CNRS, CINAM, Campus de Luminy, Université Aix Marseille, France

<sup>g</sup>Laboratoire de Biophysique, Faculté de Médecine de Monastir, Tunisie

<sup>h</sup>Laboratoire de Biochimie et de Toxicologie, CHU de Monastir, Tunisie

the use of inorganic nanotubes as nanocarrier systems were described<sup>22–26</sup> particularly the titanate nanotubes (Ti-Nts) which are gaining more and more attention thanks their high surface, large area volume and their tubular shape which leads to a higher cellular internalization. In the biomedical field, Ti-Nts have been investigated for their use in the radiosensitization effect as a new tool in radiation therapy for glioblastoma.<sup>27</sup> In addition, Ti-Nts were used in bone regeneration,<sup>28,29</sup> dopamine detection<sup>30</sup> and molecule vectorization.<sup>31,32</sup> To the best of our knowledge no nanocarrier system was developed to delivery genistein into glioblastoma tumor. In this study, for the first time, a genistein drug delivery system based on Ti-Nts was developed in order to prevent glioblastoma. It is expected that this system would improve the cellular uptake of genistein and then enhance its therapeutic effects on glioblastoma. Genistein-loaded-Ti-Nts were prepared by simple impregnation method in ethanol genistein solution. Further, theurapeutic effect of genistein-loaded-Ti-Nts was performed on U87-MG glioblastoma cells by the study of cytotoxicity and anti-migratory effects.

## Materials and methods

### Materials

Methanol (HPLC [high-performance liquid chromatography]-grade), absolute ethanol, genistein powder with about 98% purity (HPLC-grade) and 3-(4,5-dimethylthiazol-2-yl)-2,5-diphenyltetrazolium bromide (MTT) were purchased from Sigma-Aldrich France.

### Ti-Nts synthesis

Ti-Nts were synthesized as reported previously. Briefly 1.5 g of anatase  $\text{TiO}_2$  powder was added into 50 mL of 10 M aqueous NaOH solution and the obtained suspension was hydrothermally treated in a sealed Teflon autoclave at 150 °C for 5 h. The resulting precipitate was ground and dispersed in deionized water. The obtained suspension was treated with a 0.1 M HCl solution until pH value reached 2.5 and then stirred for 2 h. The filtrated white precipitate was repeatedly washed with distilled water until the pH value reached 6–7, and the product was dried at 60 °C for 48 h.

### Characterization and stability study

**Particle size, surface charge and surface morphology.** The nanotubes size and zeta potential were determined by Malvern Mastersizer 2000 (Zetasizer Nano ZS90, Malvern Instruments Ltd., UK). Before measurement, the freshly prepared Ti-Nts were appropriately suspended in pure water and sonicated for 10 min. All measurements were performed at room temperature after equilibration for 10 min. The data were obtained with the average of three measurements.

**X-ray diffraction (XRD).** X-ray powder diffraction was performed at room temperature with an X-ray diffractometer (X'Pert PRO MPD, PANalytical Co., Holland). Monochromatic Cu K $\alpha$ -radiation ( $\lambda = 1.5418 \text{ \AA}$ ) was obtained with a Ni-filtration and a system of diverging and receiving slides of 0.5° and 0.1

mm, respectively. The diffraction pattern was measured with a voltage of 40 kV and a current of 30 mA over a 2 $\theta$  range of 3–40° using a step size of 0.02° at a scan speed of 1 s per step.

**Thermogravimetric analysis.** The thermogravimetric analysis (TGA) was carried out using a SHIMADZU TGA-50 thermooanalyser instrument under an air flow of 25 mL min<sup>-1</sup>. In each case, the samples (about 5 mg of Ti-Nts) were heated from room temperature (30 °C) to 600 °C at a linear heating rate of 10 °C min<sup>-1</sup>.

### Stability study

The stability of Ti-Nts was studied in both ultra pure water and DMEM cell culture medium. Ti-Nts (5 mg/100 mL) was suspended in water or DMEM medium then sonicated for 10 min. The nanotubes were incubated in 37 °C under continuous stirring up to 30 days. Samples of 0.5 mL were collected at 1, 2, 7, 15, 21 and 30 days after centrifugation of Ti-Nts at 14 500 rpm for 15 min. After each sample collect the mediums were replaced by 0.5 mL of fresh ultrapure water or DMEM incubated at 37 °C.

### In vitro cytotoxicity of Ti-Nts and MTT assay

Ti-Nts cytotoxicity was assessed on human glioblastoma cancer cells (U87-MG cells). U87-MG cells were provided by the American Type Culture Collection. U87-MG cells line were cultured in DMEM medium containing 10% of fetal bovine serum, 1% (v/v) antibiotics (penicillin–streptomycin), and 1% glutamine in 25 cm<sup>2</sup> flasks. Cells were incubated under 37 °C with 5% CO<sub>2</sub> in a humidified incubator. For cytotoxicity study, DMEM medium was removed and the cell monolayer was washed rapidly with 3 mL of phosphate buffered saline (PBS) and then incubated in 0.5 mL of 0.05% trypsin containing 1 mM ethylenediamine tetra acetate (EDTA). After 5 min of incubation at 37 °C, the dissociated cells were collected into a tube. The tissue culture flask was washed with 4 mL of culture medium which was combined with the cell suspension. From the 5 mL of cell suspension that was recovered, a volume of 0.2 mL was removed and the cells were counted using a Beckman Coulter Z2 Counter. Typical suspension cell densities were in the range of 0.9–1.3 × 10<sup>6</sup>/mL. U87-MG cells were seeded in 96-well plates at 5000 cells per well respectively. After 24 h of cells incubation, the culture media were replaced by 150  $\mu\text{L}$  of fresh ones containing different concentrations of Ti-Nts (0.00, 0.575, 1.15, 3.37, 6.75, 12.50, 25.00, 50.00 and 100  $\mu\text{g mL}^{-1}$ ). Following incubation for 72 h, the cell viability was determined by MTT 3-(4,5-dimethylthiazol-2-yl)-2,5-diphenyltetrazolium bromide colorimetric assay as described previously.<sup>33</sup>

### Kinetics of cellular uptake of Ti-Nts

The Ti-Nts cell internalization was studied by TEM and ICP-MS through the determination of intracellular level of Ti. U87-MG cells were seeded in 6-well plates at 117 500 cells per well. After 24 h of cells incubation, the cell DMEM cell culture media were replaced by 1.5 mL of fresh medium containing 100  $\mu\text{g mL}^{-1}$  of Ti-Nts and incubated for 1 h, 3 h, 24 h, 48 h and 72 h. An equivalent cell number, used as control, was incubated

in DMEM medium without Ti-NTs. After different times of incubation with Ti-NTs, the DMEM medium was removed and cells were washed with PBS and fixed with glutaraldehyde 2.5% in 0.1 M sodium cacodylate buffer, pH 7.4 for 3 h at room temperature. Then, cells were strapped in each well and the pellets were washed three times with 0.1 M sodium cacodylate buffer, pH 7.4. The pellets were then post-fixed with 2% osmium tetroxide in 0.1 M sodium cacodylate buffer for 1 h. Pellets were then dehydrated in series of graded ethanol solutions, filtrated, and embedded in agar 100 epoxy resin, using propylene oxide as a transitional fluid. Next, ultrathin sections were cut from dried blocks with a diatom diamond knife on an LKB ultramicrotrom Leica UCT and stained with 0.5% aqueous uranyl acetate followed by Reynold's lead citrate. Finally, the sections were examined using Tecnai G2 at 200 kV (FEI, Netherland) transmission electron microscope and acquire with a Vela camera (Olympus, Japan).

### Genistein-Ti-Nts loading

Genistein was entrapped into the titanate nanotubes by suspending the powder solids (5 mg) in an ethanol solution of genistein (10 mM) at room temperature under magnetic stirring for 24 h. Prior to the encapsulation, titanate nanotubes were dehydrated at 100 °C for 12 hours in order to remove residual solvent into the pores. The Ti-Nts containing-genistein were recovered by centrifugation at 14 500 rpm for 15 min. The encapsulated genistein amount was quantified by TGA and High Performance Liquid Chromatography (HPLC). Additionally, solids were characterized by XRD before and after the genistein encapsulation.

### Genistein release

Genistein release was carried out by soaking the drug-loaded powder in a phosphate buffer solution (PBS; 0.04 M, pH 7.4) at 37 °C under bidimensional continuous stirring (120 rpm, incubator Multiton Orbitale, Infors HT, France). At different incubation times, an aliquot of supernatant (100 µL) was recovered by centrifugation (14 500 rpm, 10 min) and replaced by the same volume of PBS at 37 °C. The amount of released genistein was determined by combining HPLC and TGA methods.

### HPLC assay of genistein

HPLC (LC 1200, Agilent Technologies, Santa Clara, CA, USA) was used to determine both drug loading and encapsulation efficiency of genistein-loaded Ti-Nts. Indeed, after sample centrifugation at 14 500 rpm for 10 min the supernatant was separated and stored at -20 °C for later HPLC analysis. HPLC analysis was performed using a reverse-phase C-18 column (150 × 4.6 mm; pore size, 5 µm; Agilent Technologies) at 25 °C to determine the amount of encapsulated genistein at 262 nm. Methanol/water (60/40, v/v) was used as the mobile phase at a flow rate of 1 mL min<sup>-1</sup>. The amount of genistein was calculated according to a standard genistein sample.

### Transwell migration assay

U87-MG (50 000 cells per condition) were poured on the upper side of a transwell migration chamber (0.8 µm filter, Becton Dickinson, Le Pont de Claix, France) in serum free medium. The lower side of the chamber was filled with standard culture medium for U87 cells. Cells were allowed to transmigrate for 6 h and then chambers were removed. Cells that did not migrate stayed on the upper part of the filter and were removed with a cotton stick; cells on the lower side of the filter were fixed with 1% glutaraldehyde (Sigma-Aldrich) and stained with 1% crystal-violet solution in 20% methanol. After washing and drying, pictures of four fields per filter were taken at a magnification of 10×. Quantification of cell transmigration was made with Metamorph software® and results were expressed as percent of cells that transmigrated (mean ± SD). More than three independent experiments were performed.

### Statistical analysis

All experiments were repeated at least three times unless otherwise stated. All data are expressed as the mean ± SD. Student's *t*-test statistical analysis was performed with SPSS 16.0 software. Asterisks indicate significant level vs. control \*\* *p* < 0.05.

## Results and discussion

### Ti-Nts characterization and stability

Ti-Nts powder were milled then dispersed and sonicated in ultra-pure water. After filtration on 0.2 µm pore size membrane filter, the filtrated Ti-Nts suspension was analyzed for morphology and size distribution. Transmission electron microscopy analysis (Fig. 1A and B) showed that titanate nanomaterials have typical morphology of multiwalled nanotubes (Fig. 1B, yellow arrows) with size of 10 nm in outer diameter and 4 nm in inner diameter and the mean length is around 100–150 nm as confirmed also by dynamic light scattering (DLS) measurement (Fig. 1C). In addition the aqueous nanotubes suspension showed an homogeneous monodisperse nanoparticle system according to the polydispersity index value (PDI = 0.2) which make them particularly attractive for use in drug delivery. Moreover according to the zeta potential measurement, Ti-Nts were negatively charged (-39.7 mV) indicating a stable nanomaterial suspension. The XRD pattern of the synthesized Ti-Nts (Fig. 1D) is matches well with standard diffractogram of  $\text{H}_4\text{O}_6\text{Ti}_2$  (JCPDS card: 47-0124), which coincides with the general molecular formula of protonated titanate ( $\text{H}_2\text{TiN}\text{O}_{2n+1} \cdot x\text{H}_2\text{O}$ ).<sup>34</sup> No layered anatase  $\text{TiO}_2$  precursor can be observed in the view field. Results above indicate that the anatase  $\text{TiO}_2$  has converted to titanate with nanotube morphology entirely.

The long-term stability of Ti-Nts was studied at 37 °C in ultra-pure water and DMEM cell culture medium under continuous stirring up to 30 days. The Ti concentration was determined by ICP-MS in the samples supernatants after centrifugation at 14 500 rpm. As shown in (Fig. 1E and F) the level of Ti released

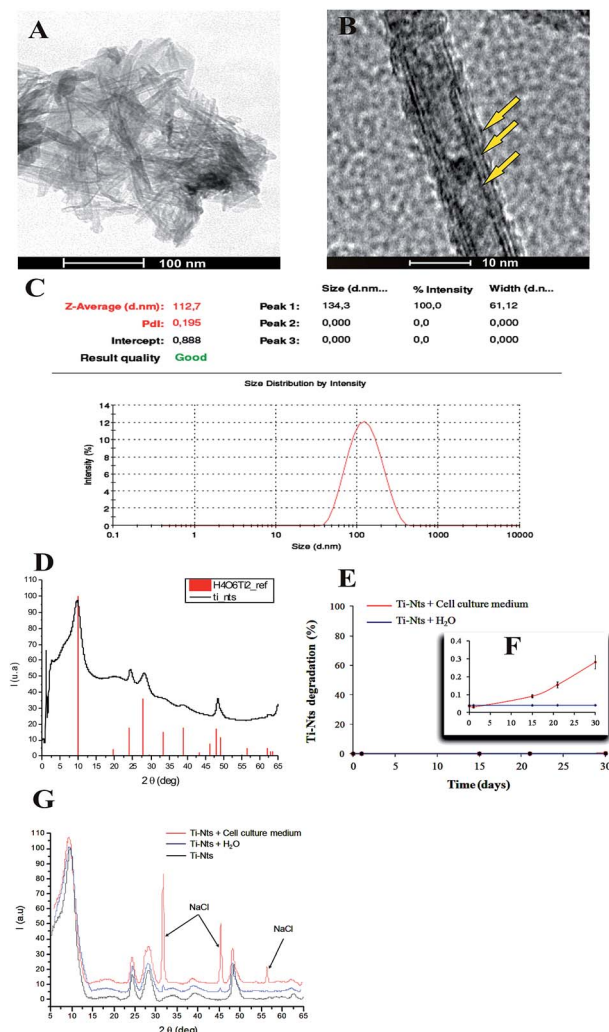


**Fig. 1** (A and B) TEM images of titanate nanotubes, (B) is a magnification of (A). (C) DLS measurement of Ti-Nts suspension in water. (D) XRD pattern of titanate nanotubes. (E and F) Stability of titanate nanotube in both aqueous solution and DMEM cell culture medium after 30 days of stirring under  $37^{\circ}\text{C}$ , (F) is a magnification of (E). (G) XRD pattern of incubated titanate nanotubes in water and DMEM for 30 days under  $37^{\circ}\text{C}$ , compared with XRD pattern of non incubated titanate nanotubes.

from degraded nanotubes was very low during 30 days showing that Ti-Nts are stable in both medium. Moreover no morphological changes in the Ti-Nts crystalline structure were observed as confirmed by XRD (Fig. 1G) except the presence of new peaks at 31, 45 and 55 degree for Ti-Nts incubated in DMEM medium. These peaks are attributed to the NaCl containing medium as confirmed by standard diffractogram of NaCl.<sup>34</sup>

### Cytotoxicity of Ti-Nts

U87-MG cells were adopted to assess the cytotoxicity of Ti-Nts. Ti-Nts were suspended and sonicated for 10 min in the DMEM cell culture medium then the suspension were subjected to gamma radiation sterilization. No significant changes in the size and PDI parameters of Ti-Nts-DMEM suspension as confirmed by DLS measurement.

Ti-Nts suspensions at concentrations ranging from 0.575 up to  $100 \mu\text{g mL}^{-1}$  were incubated with U87-MG cells for 72 h. As shown in Fig. 2, the U87-MG cell viability profile did not show any obvious cytotoxicity up to the higher concentration ( $100 \mu\text{g mL}^{-1}$ ). The inhibition of cell survival was below 20% excluding the toxicity effects of Ti-Nts. Taken together these results approved the safety of Ti-Nts and allowed their use in the biomedical applications.

### Kinetics of cellular uptake of Ti-Nts

Kinetics of Ti-Nts cell internalization was studied by TEM and ICP-MS. Indeed ICP-MS was used to determine the intracellular concentration of titanium after 1, 4, 24, 48 and 72 h of U87-MG cells incubation with Ti-Nts ( $100 \mu\text{g mL}^{-1}$ ). As shown in the Table 1, the intracellular titanium concentration increased from 1 h up to 48 h in U87-MG cells to achieve an average concentration of  $60.32 (\pm 6.30) \mu\text{g mg}^{-1}$  of cellular proteins. Moreover the intracellular content of Ti-Nts was statistically unchanged following 48 h and 72 h of incubation suggesting Ti-Nts-cells uptake saturation.

TEM observations showed a high cell internalization of Ti-Nts in a majority of cells as a direct consequence of their tubular shape (more than 80% of cells have internalized following 48 h of cell incubation). After 1 h of Ti-Nts/cells incubation the nanotubes were located inside vesicles (Fig. 3, yellow arrow) or escaping from vesicles into the cytosol (Fig. 3, red arrow). Note that in control cells, similar vesicles into the cytosol are empty of Ti-Nts (Fig. 3, yellow arrow). It can be concluded that two internalization pathways were occurred simultaneously: endocytosis (Fig. 3, 48 h dotted red arrow) with invagination of the membrane and a diffusion process. The presence of nanostructures outside the U87-MG cells despite the washing steps suggests the possible exocytosis of Ti-Nts (Fig. 3, 48 h).

The amount of intracellular Ti-Nts increased slowly until 48 h of incubation with U87-MG cells suggesting time dependent cellular uptake as confirmed by ICP-MS (Table 1). The morphology of cell organelles including nucleus and mitochondria was normal during the incubation time compared to the control cells, indicating the absence of Ti-Nts toxic effect.

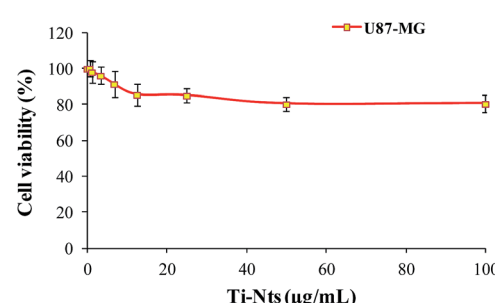


**Fig. 2** Cell viability of U87-MG determined by MTT assay after 72 h of incubation with different concentrations of Ti-Nts ranging from 0.5 to  $100 \mu\text{g mL}^{-1}$ . Each data point corresponds to mean values of four experiments (results shown are representative curves from three independent experiments).

**Table 1** Intracellular concentration of titanium determined by ICP-MS in U87-MG cells following 1, 4, 24, 48 and 72 h of incubation with 100  $\mu\text{g mL}^{-1}$  of Ti-Nts. Results are representative of three independent experiments

Time of cells incubation with Ti-Nts	[Ti] ( $\mu\text{g mg}^{-1}$ of cellular proteins)
1 h	10.42 ( $\pm 3.64$ )
4 h	23.6 ( $\pm 4.84$ )
24 h	35.25 ( $\pm 5.23$ )
48 h	60.32 ( $\pm 6.30$ )
72 h	60.02 ( $\pm 7.12$ )

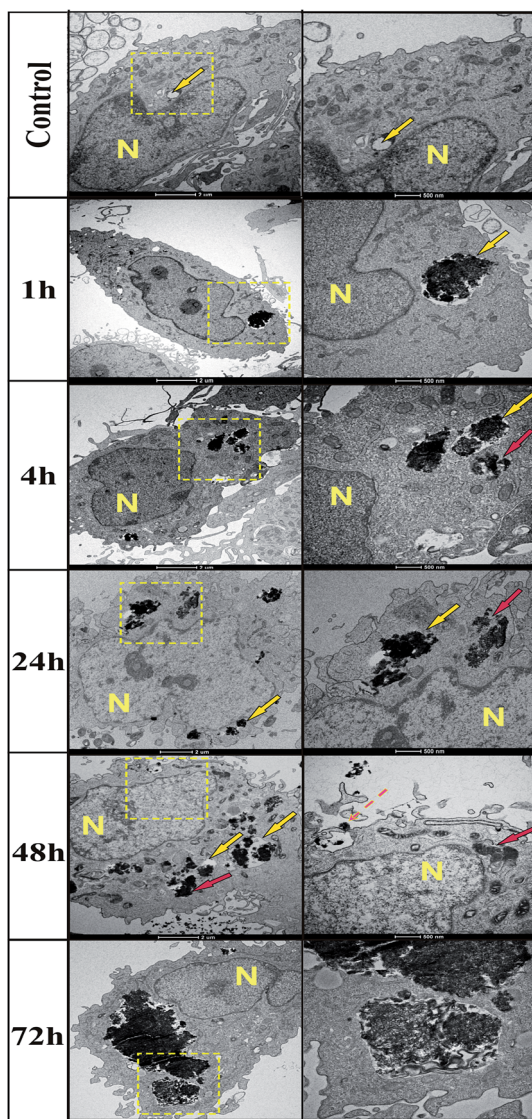


**Fig. 3** TEM images of Ti-Nts internalization into U87-MG after 1, 4, 24, 48, and 72 h of incubation with 100  $\mu\text{g mL}^{-1}$ . Nanotubes were located inside vesicles (yellow arrow) or escaping from vesicles into the cytosol (red arrow). Ti-Nts were located outside the cells (48 h, dotted red arrow) into invaginations of the plasma membrane. (N = nucleus).

After 72 h of incubation, giant U87-MG cells with strong accumulation of intracytoplasmic nanotubes can be normally observed as a sign of abnormal mitosis. In addition a slight cell swelling is characterized by the fusion of endosomes containing Ti-Nts to form large vesicle confirming Ti-Nts/cells saturation without membrane destruction or cellular apoptosis.

### Genistein-Ti-Nts loading and release

Genistein loading was carried out by a simple impregnation method by suspending the milled Ti-Nts powder (5  $\text{mg mL}^{-1}$ ) into nontoxic ethanol genistein solutions (2.5  $\text{mg mL}^{-1}$ ) for 24 h. The kinetics of genistein-Ti-Nts loading was studied at 0.5, 1, 3, 6, 8, 12 and 24 h by the determination of the genistein concentration in the supernatant after sample centrifugation at 14 000 rpm. The results show a high genistein payload (Fig. 4A). The optimal encapsulation efficiency and drug loading of the genistein-Ti-Nts determined by HPLC were  $50.4\% \pm 1.41\%$  and  $25.2\% \pm 1.04\%$ , respectively. Moreover the level of genistein containing Ti-Nts did not change significantly after 12 h of entrapment, suggesting saturation of multiwalled Ti-Nts pores. In order to confirm these results, TGA was employed to measure the amount of the final genistein loading in the Ti-Nts. Typical thermograms of empty Ti-Nts and genistein-Ti-Nts complex are reported in Fig. 4B. Indeed the empty Ti-Nts dehydrate at the low temperatures (50–300 °C, weight loss: 11.2 wt%). However the TGA curves of the Ti-Nts containing genistein shows two different weight losses. In detail the first weight loss, between 50 and around 300 °C, is due to the departure of water and ethanol, the second one more differentiated (from 300 to 350 °C) corresponds to the genistein departure. The amount of genistein was estimated considering the weight losses of the empty dried Ti-Nts (mg of genistein per 100 mg of dry Ti-Nts). Indeed a large genistein payload up to 51.6 wt% was achieved in Ti-Nts confirming the results obtained by HPLC.

Moreover crystalline structures of Ti-Nts, genistein-Ti-Nts complex and pristine genistein were checked by XRD (Fig. 4C). XRD patterns of empty Ti-Nts and genistein-Ti-Nts show that impregnation step does not alter their crystalline structure. In addition a significant change in the relative Bragg peaks intensity was observed suggesting the filling of Ti-Nts pores by genistein molecules Fig. 4C (arrows). Remarkably, no recrystallized genistein is observed whatever on the Ti-Nts surface, as confirmed by XRD.

Concerning the drug release, a biphasic drug release of the genistein is observed with no “burst effect” Fig. 4D. Indeed the level of genistein is progressively released from Ti-Nts in the PBS to achieve 25% up to 3 h then increased linearly to achieve 80% after 72 h.

After 6 days 95% of the encapsulated genistein were released. The comparison between kinetics of genistein delivery and the kinetics of Ti-Nts degradation suggests that the delivery process is governed mainly by diffusion from the pores and/or drug-matrix interactions and not by the Ti-Nts degradation. Indeed, the total delivery of Ti-Nts occurred within 6 days, when only approximately 0.05% of Ti-Nts were degraded.

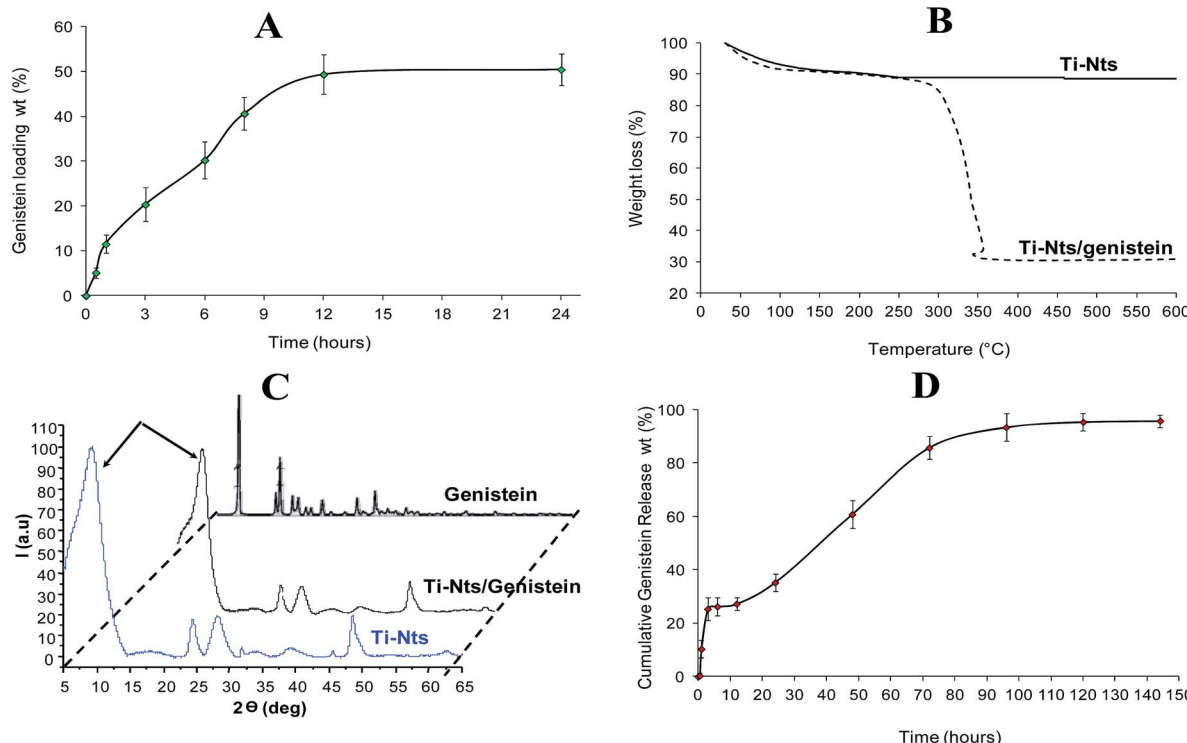


Fig. 4 (A) kinetic of genistein encapsulation into Ti-Nts at room temperature (B) TGA thermograms of empty Ti-Nts and genistein-loaded Ti-Nts (C) XRD patterns of empty Ti-Nts, genistein-loaded-Ti-Nts and free genistein (D) genistein release from Ti-Nts under simulated physiological conditions (PBS, 37 °C). All experiments were carried out in triplicate.

### Cytotoxicity of pristine genistein *versus* genistein-loaded-Ti-Nts on U87-MG cells

Before cells treatment, both the size distribution and the zeta potential of genistein-loaded-Ti-Nts suspension in the PBS were measured. The surface charge of genistein-loaded-TiNts increased to be  $-31.9$  mV as compared with the charge of the empty Ti-Nts ( $-39.7$  mV). Moreover the genistein-loaded-TiNts suspension showed a relatively high distribution and stability (PDI = 0.23), which make them a perfect delivery system. U87-MG cells were treated with pristine genistein ( $25.2 \mu\text{g mL}^{-1}$ ) or its equivalent of genistein-loaded Ti-Nts ( $100 \mu\text{g mL}^{-1}$ ) or

empty Ti-Nts ( $100 \mu\text{g mL}^{-1}$ ) for 24 h. As shown in Fig. 5 the cells viability declined significantly with genistein and genistein-loaded-Ti-Nts treatment 32% and 60% respectively. Whereas U87-MG cells treated with empty Ti-Nts show no significant viability reduction as compared with the control. The genistein-loaded-Ti-Nts did show much higher cytotoxicity efficacy against U87-MG cells than the pristine genistein after 24 h of incubation indicating higher therapeutic efficacy for U87-MG cells.

This may be attributed to the higher cellular uptake of genistein-loaded Ti-Nts followed by the faster genistein release as a consequence of the intracellular degradation conditions.

Further, the ultra-structure of cells was examined by TEM (Fig. 6). The Ti-Nts were observed inside vesicle (yellow arrow) and into the cytosol (red arrow). Treatment with free genistein or genistein-loaded-Ti-Nts lead to various abnormalities in mitochondrial structure, and cristae organization, compared with the mitochondria of cells treated with empty Ti-Nts. Indeed the mitochondria of cells treated with empty Ti-Nts maintained the morphology of normal conformation in healthy cells (Fig. 6). However, after treating with genistein-loaded-Ti-Nts or free genistein, unusual morphologies and serious damage of mitochondria were observed. Indeed several mitochondria showed irregular swelling and severe vacuolization (Fig. 6, red arrows). Moreover, some of the mitochondrial membrane was broken which was considered for leaking out of the mitochondrial matrix.

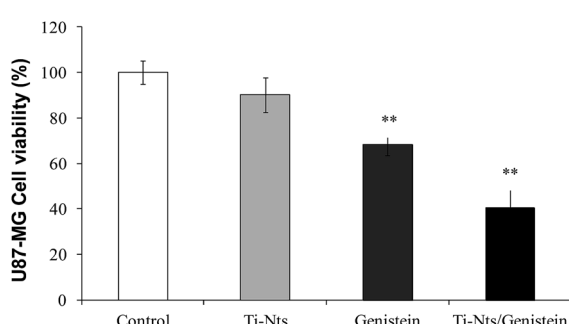
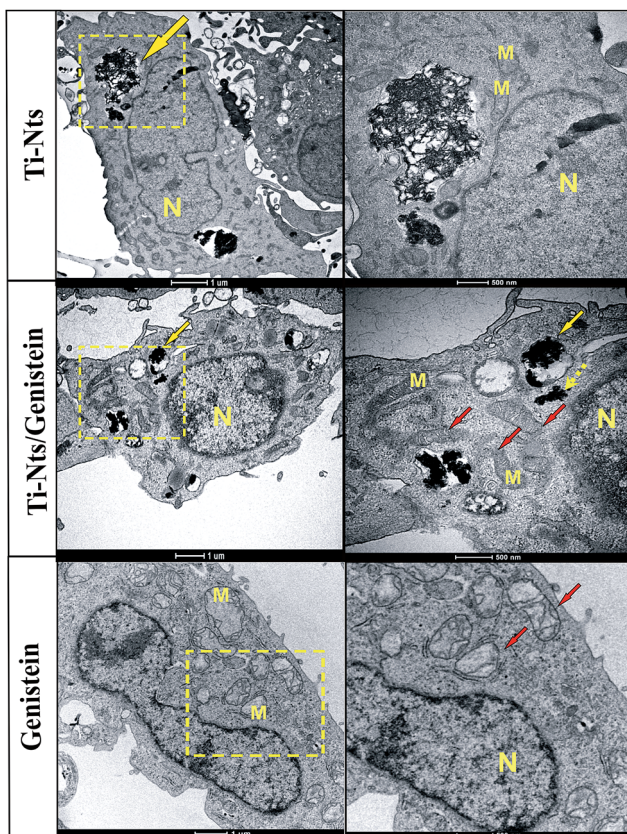


Fig. 5 Viability of U87-MG cells incubated for 72 h with Ti-Nts ( $100 \mu\text{g mL}^{-1}$ ) or genistein ( $25.2 \mu\text{g mL}^{-1}$ ) or genistein-loaded Ti-Nts ( $100 \mu\text{g mL}^{-1}$ ) in comparison with the control. Mean and standard deviation for triplicate experiments were reported. Significance was indicated by: \*\*  $p < 0.05$ .



**Fig. 6** TEM images of U87-MG incubated for 24 h with Ti-Nts ( $100 \mu\text{g mL}^{-1}$ ), genistein-loaded Ti-Nts ( $100 \mu\text{g mL}^{-1}$ ) and free genistein ( $25.2 \mu\text{g mL}^{-1}$ ). Nanotubes were located inside vesicles (yellow arrow) or escaping from vesicles into the cytosol (dotted yellow arrow). Treatment with free genistein or Ti-Nts/genistein lead to various abnormalities in mitochondrial structure (red arrow) and cristae organization, compared with the mitochondria of cells treated with empty Ti-Nts. (N = nucleus, M = mitochondria).

### Anti-migration effects of genistein-loaded-TiNts on U87-MG cells

Genistein ( $25.2 \mu\text{g mL}^{-1}$ ) or Ti-Nts ( $100 \mu\text{g mL}^{-1}$ ) or genistein-loaded-Ti-Nts complex ( $100 \mu\text{g mL}^{-1}$ ) were added in both upper and lower side of the transwell chamber. Cells were allowed to transmigrate for 6 h and then chambers were removed. As shown in Fig. 7, in comparison with the control cells, the genistein and genistein-loaded-Ti-Nts decreased significantly the cell migration with 19.90% and 39.69% respectively. Whereas Ti-Nts did not show significant inhibition (only 4.3%). Interestingly the inhibitory effect of genistein delivered by Ti-Nts on cell migration is higher than the one of pristine genistein. These results show that inhibitory cell migration effect is correlated with the level of genistein cell uptake and confirming that genistein cellular uptake and diffusion was more efficient when delivered by Ti-Nts.

## Discussion

In this study, the characterization of titanate nanotubes, their safety and their potential to encapsulate genistein were

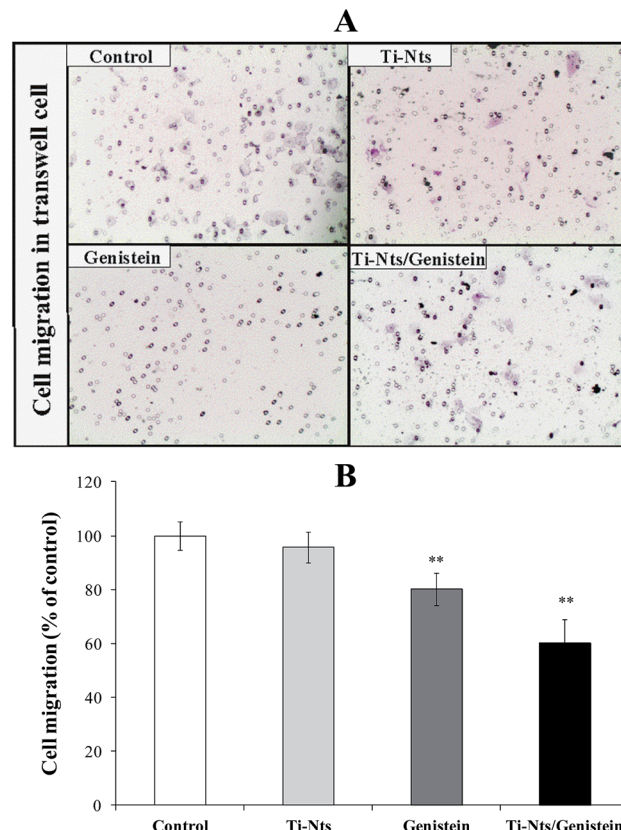


**Fig. 7** (A) Representative images of migratory U87-MG cells using the transwell migration assay (crystal violet staining, magnification of  $100\times$ ). (B) Quantification of migratory cells treated with genistein ( $25.2 \mu\text{g mL}^{-1}$ ), Ti-Nts et Ti-Nts/genistein ( $100 \mu\text{g mL}^{-1}$ ) or not (control) expressed as percentage of 100% control cells determined by counting the cell number under the microscope (magnification of  $100\times$ ) in the transwell migration assay. Three independent experiments were performed for each condition. Bar  $\pm$  SEM. (\*) indicates significant differences from control: \*\*  $p < 0.05$ .

investigated. Moreover the genistein-loaded-Ti-Nts was tested for their cytotoxicity and anti-migratory effect on U87-MG cells line.

The biocompatibility of Ti-Nts was investigated on U87-MG cells at the higher concentration  $100 \mu\text{g mL}^{-1}$ . Very few studies have been reported on the cytotoxicity of Ti-Nts in the literature. The cytotoxicity of  $\text{TiO}_2$ -based nanofilaments was reported on H596 lung carcinoma cells for a concentration  $2 \mu\text{g mL}^{-1}$  depending on their morphology and chemical composition.<sup>35</sup> In addition Ti-Nts did not show any toxicity on neonatal cardiomyocytes after 24 h of incubation with different concentrations ( $0$ – $10 \mu\text{g mL}^{-1}$ ).<sup>33</sup> Despite that nanoparticles cytotoxicity is highly dependent on the cell type,<sup>36</sup> our results shows that Ti-Nts are biocompatible after 3 days of exposition to U87-MG cells at a concentration 10 and 50 times higher than the concentrations reported for neonatal cardiomyocytes and H596 lung carcinoma cells respectively.<sup>32,35</sup> Similar cytotoxicity results were obtained for Ti-Nts used in the radiosensitization for glioblastoma therapy.<sup>27</sup> Concerning the pathway of Ti-Nts cells internalization, two processes were evidenced by TEM: through endocytosis, with cell membrane invagination and via direct

penetration through the bilayer, as reported in the case of carbon nanotubes<sup>37</sup> and of Ti-Nts into cardiomyocytes.<sup>32</sup>

Particle size and surface characteristics of the nanoparticles play a vital role in drug release kinetics, cellular uptake behavior as well as *in vivo* pharmacokinetics and tissue distribution.<sup>38</sup> The average hydrodynamic diameter of the genistein-loaded-Ti-Nts is approximately 120–150 nm, which is in the excellent size range for accumulating readily in tumor vasculature due to the enhanced permeation and retention effects.<sup>39</sup> Likewise the PDI of both empty Ti-Nts and genistein-load-TiNts is around 0.2 indicating that the size distribution of the nanomaterials was a relatively narrow particle size distribution and have a uniform size which makes them particularly attractive for use in drug delivery system as reported for nanoparticles.<sup>39</sup> It can be noted that the mean size and size distribution of the genistein-loaded Ti-Nts were almost not changed during a week after redispersion in DMEM medium, indicating that genistein-loaded-Ti-Nts exhibited good redispersion ability, without increasing the average diameter and a good stability over time. The zeta potential is a key indicator of the stability of colloidal dispersions. High absolute value of the zeta potential means high surface charge of the nanoparticles. The zeta potential of the genistein loaded-Ti-Nts was determined to be –31.9 mV which is slightly higher than that of the empty Ti-Nts (–39.7 mV). The negative surface charge of Ti-Nts may be due to the presence of hydroxyl groups. It was reported that the zeta potential of colloidal carriers was above the critical value of –30 mV, implying the good stability.<sup>39</sup>

Many models of nanocarriers have been developed for genistein delivery such as copolymer mannitol-functionalized PLGA-TPGS for liver cancer treatment,<sup>40</sup> Flt1 peptide–hyaluronate conjugate micelle-like nanoparticles for the treatment of ocular neovascularization<sup>41</sup> or nanostructured lipid carriers for the prevention of posterior capsular opacification.<sup>42</sup> All these organic nanocarriers have a spherical shape and each has its own chemical and biological functions. It is known that cellular uptake of tubular nanocarriers is higher than spherical nanocarriers as demonstrated for TiO<sub>2</sub> based nanofilament in comparison with spherical titanium oxide nanoparticles (P25).<sup>32,35</sup>

Interestingly these organic nanocarriers are not able to be used for glioblastoma treatment as a consequence to their low stability in the biological medium or to their burst drug release. Moreover surface chemical properties of these nanoparticles allows to a low affinity to the blood brain barrier. Thanks to its external chemical surface, the inorganic Ti-Nts could present new options as well as various graftings *via* the available hydroxyl groups,<sup>43</sup> and the tubular shape which gives different penetration characteristics compared with nanospheres. Moreover, the hydrophobicity of Ti-Nts leads to a better affinity to the blood brain barrier and a high stability in biological medium for long time which is perfect for drug encapsulation and release.

The advantages in cancer cell inhibition of the genistein-loaded Ti-Nts could be quantitatively demonstrated in terms of their half maximal inhibitory concentration (IC<sub>50</sub>) values, which is defined as the drug inhibitory concentration that is required to cause 50% cancer cell mortality in a designated

period. The IC<sub>50</sub> values of U87-MG cells after 24 h incubation with free genistein and genistein-loaded-Ti-Nts are shown in Fig. 5. It can be found that the IC<sub>50</sub> value of the genistein-loaded Ti-Nts for U87-MG cells was 31.18 µg mL<sup>–1</sup>, which was a degree higher than pristine genistein (18.46 µg mL<sup>–1</sup>) after 24 h incubation. It is concluded that the genistein-loaded nanoparticles exhibited significantly higher cytotoxicity for U87-MG cells owing to the sustained drug release manner. Further the released genistein level from Ti-Nts after 6 hours is theoretically 6.3 µg mL<sup>–1</sup> as we demonstrated in PBS. However the inhibitory effect of genistein-loaded-Ti-Nts on U87-MG migration (39.7%) was higher than the one of free genistein at the concentration 25.5 µg mL<sup>–1</sup>. This result is correlated with the high cellular uptake of genistein-loaded-Ti-Nts as confirmed by TEM and suggesting a fast diffusion of the drug into the cytosol under hard biological condition to act on the mitochondria. Indeed it is known that pharmacological anticancer activities of genistein involve the inhibition of G2/M cell cycle phase and deregulation of mitochondrial membrane pore permeability.<sup>44,45</sup>

## Conclusion

A novel biocompatible nanocarrier system based on titanate nanotubes for sustained and controlled delivery of genistein for the prevention of glioblastoma was developed in this study. The safety of Ti-Nts was proved on U87-MG cells at higher concentration up to 100 µg mL<sup>–1</sup>. The genistein-loaded-Ti-Nts formulations were fabricated by a sample entrapment method in ethanol genistein and were stable in cell culture medium for 3 days. The particle size of genistein-loaded-Ti-Nts is in the range of 110–150 nm in length and 10 nm approximately in outer diameter. The Ti-Nts could achieve higher genistein drug-loading content (25.2%) and entrapment efficiency (51.2%) leading to controlled drug release as well as higher cellular uptake, cytotoxicity and significant anti-migratory effect on U87-MG promising efficient antitumor activity. Future work will investigate the pathway and mechanism of the cellular uptake then study the efficacy of genistein-loaded-Ti-Nts to prevent glioblastoma *in vivo*. The great advantages of Ti-Nts can also be used to other drugs of difficulty in formulation owing to high hydrophobicity.

## Acknowledgements

The work was supported by the Tunisian National Institute of Research and Physicochemical Analysis "INRAP, technopole Sidi Thabet Ariana. We acknowledge the support of the Tunisian Ministry of Higher Education and Scientific Research.

## References

- 1 M. Sanchez-Martin, *Curr. Stem Cell Res. Ther.*, 2008, **3**, 197–207.
- 2 P. Y. Wen and S. Kesari, *N. Engl. J. Med.*, 2008, **5**, 492–507.
- 3 H. K. Wang, *Expert Opin. Invest. Drugs*, 2000, **9**, 2103–2119.

- Published on 19 October 2016. Downloaded by Pontifícia Universidade Católica do Rio Grande do Sul on 8/27/2024 7:57:02 PM.
- 4 T. Valachovicova, V. Slivova and D. Sliva, *Mini-Rev. Med. Chem.*, 2004, **4**, 881–887.
  - 5 Y. Sánchez, C. Calle, E. Blas and P. Aller, *Chem.-Biol. Interact.*, 2009, **182**, 37–44.
  - 6 O. J. Bandele and N. Osheroff, *Biochemistry*, 2007, **46**, 6097–6108.
  - 7 A. M. Azarova, R. K. Lin, Y. C. Tsai, L. F. Liu, C. P. Lin and Y. L. Lyu, *Biochem. Biophys. Res. Commun.*, 2010, **399**, 66–71.
  - 8 D. Li, J. A. Yee, M. H. McGuire, P. A. Murphy and L. Yan, *J. Nutr.*, 1999, **129**, 1075–1078.
  - 9 M. F. Aguero, M. Venero, D. M. Brown, M. E. Smulson and P. Espinoza, *Prostate*, 2010, **70**, 1211–1221.
  - 10 A. Das, N. L. Banik and S. K. Ray, *Cancer*, 2010, **116**, 164–176.
  - 11 S. Puli, J. C. Lai and A. Bhushan, *J. Neuro-Oncol.*, 2006, **79**, 135–142.
  - 12 P. L. Penar, S. Khoshyomn, A. Bhushan and T. R. Tritton, *Neurosurgery*, 1997, **40**, 141–151.
  - 13 K. D. R. Setchell, *Am. J. Clin. Nutr.*, 1998, **68**, 1333–S1346.
  - 14 J. S. Yakisich, Å. Sidén, V. I. Vargas, P. Enero and M. Cruz, *Exp. Neurol.*, 1998, **151**, 194–202.
  - 15 L. Mei, Z. Zhang, L. Zhao, L. Huang, X. L. Yang, J. Tang and S. S. Feng, *Adv. Drug Delivery Rev.*, 2013, **65**, 880–890.
  - 16 Z. P. Zhang, L. Mei and S. S. Feng, *Nanomedicine*, 2012, **7**, 1645–1647.
  - 17 F. Yan, C. Zhang, Y. Zheng, L. Mei, L. N. Tang and C. X. Song, *Nanomedicine*, 2010, **6**, 170–178.
  - 18 X. Zhang, X. Zeng, X. Liang, Y. Yang, X. Li, H. Chen, L. Huang, L. Mei and S. S. Feng, *Biomaterials*, 2014, **35**, 9144–9154.
  - 19 X. Zhang, Y. Dong, X. Zeng, X. Liang, X. Li, W. Tao, H. Chen, Y. Jiang, L. Mei and S. S. Feng, *Biomaterials*, 2014, **35**, 1932–1943.
  - 20 J. Tomasina, S. Lheureux, P. Gauduchon, S. Rault and A. Malzert-Fréon, *Biomaterials*, 2013, **34**, 1073–1101.
  - 21 X. Zeng, W. Tao, L. Mei, L. Huang, C. Tan and S. S. Feng, *Biomaterials*, 2013, **34**, 6058–6067.
  - 22 C. N. R. Rao and M. Nash, *Dalton Trans.*, 2003, **1**, 20–24.
  - 23 C. N. R. Rao, S. R. C. Vivechchand, K. Biswas and A. Govindaraj, *Dalton Trans.*, 2007, **3**, 728–749.
  - 24 K. Shankar, J. Bandara, M. Paulose, H. Wietasch, O. K. Varghese, G. K. Mor, T. J. LaTempa, M. Thelakkat and C. A. Grimes, *Nano Lett.*, 2008, **8**, 1654–1659.
  - 25 J. H. Park, S. Kim and A. J. Bard, *Nano Lett.*, 2006, **6**, 24–28.
  - 26 S. E. Gratton, P. A. Ropp, P. D. Pohlhaus, J. C. Luft, V. J. Madden and M. E. Napier, *Proc. Natl. Acad. Sci. U. S. A.*, 2008, **105**, 11613–11618.
  - 27 C. Mirjolet, A. L. Papa, G. Créhange, O. Raguin, C. Seignez, C. Paul, G. Truc, P. Maingon and N. Millot, *Radiother. Oncol.*, 2013, **108**, 136–142.
  - 28 K. S. Brammer, C. J. Frandsen and S. Jin, *Biotechnology*, 2012, **30**, 315.
  - 29 S. Kubota, K. Johkura, K. Asanuma, Y. Okouchi, N. Ogiwara, K. Sasaki and T. Kasuga, *J. Mater. Sci.: Mater. Med.*, 2004, **15**, 1031.
  - 30 S. Mahshid, C. Li, S. S. Mahshid, M. Askari, A. Dolati, L. Yang, S. Luo and Q. Cai, *Analyst*, 2011, **136**, 2322.
  - 31 R. Moumita, C. Sriparna, D. Tanmay, B. Somnath, A. Pushan and M. Shyamalava, *Nanotechnology*, 2011, **22**, 5705.
  - 32 A. L. Papa, L. Dumont, D. Vandroux and N. Millot, *Nanotoxicology*, 2013, **7**, 1131.
  - 33 T. Baati, A. Al-Kattan, M. A. Esteve, L. Njim, Y. Y. Ryabchikov, F. Chaspoul, M. Hammami, M. Sentis, A. v. Kabashin and D. Braguer, *Sci. Rep.*, 2016, **6**, 25400.
  - 34 A. R. Armstrong, G. Armstrong and J. Canales, *Angew. Chem., Int. Ed.*, 2004, **43**, 2286–2288.
  - 35 A. Magrez, L. Horvath, R. Smajda, V. Salicio, N. Pasquier and L. Forro, *ACS Nano*, 2009, **3**, 2274–2280.
  - 36 B. L'Azou, J. Jorly, D. On, E. Sellier, F. Moisan and J. Fleury-Feith, *Part. Fibre Toxicol.*, 2008, **5**, 22.
  - 37 E. Morgado, M. A. S. Abreu, O. R. C. Pravia, B. A. Marinkovic, P. M. Jardim, F. C. Rizzo and A. S. Araujo, *Solid State Sci.*, 2006, **8**, 888.
  - 38 S. D. Perrault, C. Walkey, T. Jennings, H. C. Fischer and W. C. Chan, *Nano Lett.*, 2009, **9**, 1909–1915.
  - 39 F. Yan, C. Zhang, Y. Zheng, L. Mei, L. N. Tang and C. X. Song, *Nanomedicine*, 2010, **6**, 170–178.
  - 40 W. Binquan, L. Yong, T. Yi, X. Chunmei, J. Shen, M. Zhang, X. Liu, L. Yang, F. Zhang, L. Liu, S. Cai, D. Huai, D. Zheng, R. Zhang, C. Zhang, K. Chen and X. T. Sui, *Mater. Sci. Eng., C*, 2016, **59**, 792–800.
  - 41 H. Kim, J. S. Choi, K. S. Kim, J. A. Yang, C. K. Joo and S. K. Hahn, *Acta Biomater.*, 2012, **8**, 3932–3940.
  - 42 W. Zhang, X. Li, T. Ye, F. Chen, X. Sun, J. Kong, X. Yang, W. Pan and S. Li, *Int. J. Pharm.*, 2013, **454**, 354–366.
  - 43 M. H. Razali, A. F. M. Noor, A. R. Mohamed and S. Sreekanthan, *J. Nanomater.*, 2012, **10**, 502–508.
  - 44 S. A. Alhasan, H. Pietrasczkiwicz, M. D. Alonso, J. Ensley and F. H. Sarkar, *Nutr. Cancer*, 1999, **34**, 12–19.
  - 45 S. Banerjee, Y. Li, Z. Wang and F. H. Sarkar, *Cancer Lett.*, 2008, **269**, 226–242.